PHYSICAL REVIEW E, VOLUME 65, 045402(R)

Polarization effects and anisotropy in three-dimensional relativistic self-focusing

N. M. Naumova,[1,2] S. V. Bulanov,[2] K. Nishihara,[3] T. Zh. Esirkepov,[4] and F. Pegoraro[5]
[1]*Max-Born Institute für Quantenoptik, Berlin, Germany*
[2]*General Physics Institute RAS, Moscow, Russia*
[3]*Institute of Laser Engineering, Osaka University, Osaka, Japan*
[4]*Moscow Institute of Physics and Technology, Dolgoprudny, Russia*
[5]*Department of Physics, Pisa University and INFM, Pisa, Italy*

(Received 24 December 2001; published 11 April 2002)

The relativistic self-focusing of high-intensity laser pulses in underdense plasmas is investigated with three-dimensional particle in cell simulations. The different behavior of a linearly polarized pulse in the two transverse directions is interpreted as a combination of two two-dimensional responses with different polarizations. In the polarization plane a high density sheet is formed, which separates the two regions of oppositely directed quasistatic magnetic field.

DOI: 10.1103/PhysRevE.65.045402 PACS number(s): 52.38.Hb, 52.27.Ny, 52.35.Mw, 52.65.Rr

The interaction of relativistically intense ($I > 1.35 \times 10^{18}$ W/cm^2) ultrashort laser pulses with plasmas has been investigated for many years in view of its various applications to the acceleration of charged particles [1] and to controlled nuclear fusion in the framework of the fast ignition concept [2]. For such applications to be feasible, the laser pulse interaction with the plasma must evolve in a controlled way. On the other hand, a high intensity laser pulse interacting with an underdense plasma is subject to instabilities that develop on the electron time scale and lead to a fast transformation of the pulse energy into the energy of plasma excitations. A global redistribution of the laser pulse energy inside the underdense plasma appears due to the pulse self-focusing and its filamentation instability, which are due to the relativistic increase in the electron mass and to the plasma density redistribution under the action of the pulse ponderomotive force [3–5], when the laser power exceeds (or is well above in the case of the filamentation instability) the threshold value $P_{cr} \simeq 2 m_e^2 c^5 \omega_0^2 / e^2 \omega_{pe}^2 \simeq 17(\omega_0/\omega_{pe})^2$ GW. The stimulated Raman scattering instability, which leads to the erosion of the leading edge of the laser pulse [6], is the fastest mode to develop on the electron time scale. This instability causes the formation of a steep laser front similar to a shock. Such a shock front generates a wake field, that accelerates the electrons in the plasma [7]. This leads to fast depletion of the laser pulse energy [$t_{dep} \sim (\omega_0/\omega_{pe})^2 \tau_p$] [6] and to induced focusing of the laser light behind the front [8]. Here τ_p is the pulse duration. In these regimes kinetic effects are important and the electrons accelerated inside a laser pulse that has undergone self-focussing produce electric currents in the plasma and a quasistatic magnetic field associated with them [9]. The attraction of the electric currents leads to the redistribution of the fast electrons, which in turn change the plasma refractive index. This process causes high intensity laser radiation to interact magnetically and makes the laser light filaments merge. The overall efficiency of the laser energy transport over long distances is thus controlled by the interplay of self-focusing and filament coalescence on one side and pulse depletion on the other.

The goal of the present paper is to investigate the effects of the pulse polarization and of energetic particles (i.e., of the kinetic plasma dynamics) on the nonlinear evolution of a laser pulse in an underdense plasma. In particular we will show that relativistic self-focusing and filamentation in three-dimensional (3D) configurations are anisotropic (see also Ref. [10], where small-scale anisotropic filamentation of the laser pulse has been seen in the overdense plasma).

The nonlinear evolution of an electromagnetic wave in an underdense plasma has been studied analytically [4,5] under various simplifying assumptions, such as pulse circular polarization, quasistatic approximation, and weak nonlinearity, or within the framework of the paraxial approximation [8]. Linearly polarized pulses are more complex to study because the analytic simplifications, which follow in the case of circularly polarized pulses from their lack of harmonic content, do not apply. In addition, the intensity of modern petawatt power laser pulses is so high that we cannot take advantage of the weak nonlinearity approximation. As is well known, in 3D plasma configurations the role of nonlinearity becomes more important than in 1D and 2D cases because in 3D configurations the phenomenon of wave collapse results in the development of a 3D singularity [11]. In this case the role of three-dimensional computer simulations cannot be understated.

In the present paper we study the propagation of linearly polarized, ultraintense laser pulses in underdense plasmas by using a three-dimensional particle in cell (PIC) code REMP (relativistic electromagnetic particle-mesh code). This code employs an algorithm for computing the electric current density that satisfies the charge conservation law exactly and a second order spline form factor for quasiparticles, which reduces the noise of PIC simulations dramatically [12]. The REMP code is massively parallelized and fully vectorized. We identify features of the laser light plasma interaction in three-dimensional regimes. Some of these features were described in Refs. [10,13]. In Ref. [13] it was shown that the magnetic interaction, discovered in 2D configurations in Ref. [9], plays an important role during relativistic self-focusing also in the 3D case for circularly polarized light. In Ref. [10] it was shown that an ultrashort, linearly polarized pulse breaks up into clumps, with a size of the order of the collisionless skin depth, c/ω_{pe}, both in the direction perpendicular to the pulse polarization and in the forward direction.

We consider the relativistic self-focusing of a linearly polarized semi-infinite laser beam in an underdense plasma

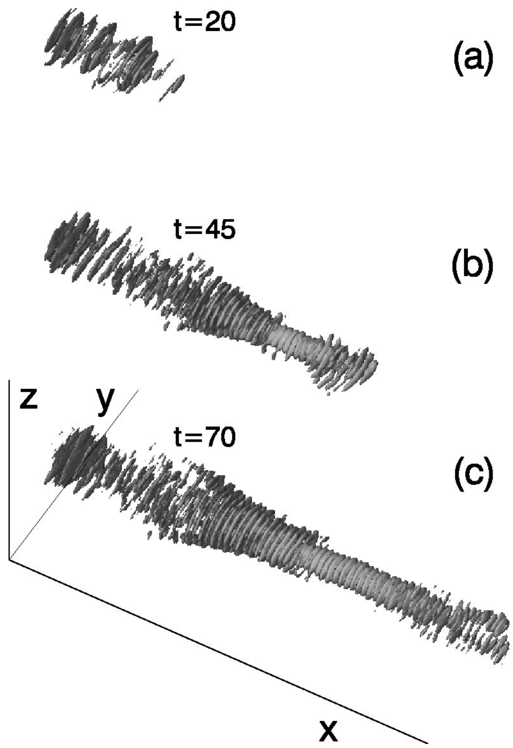

FIG. 1. 3D view of the isosurface of the electromagnetic energy density of a linearly polarized semi-infinite beam at $t=20\times 2\pi/\omega$ (a), $45\times 2\pi/\omega$ (b), $70\times 2\pi/\omega$ (c).

with the electric field in the y direction. The dimensionless amplitude of the laser pulse is $a=eE/m_e\omega c=3$, which corresponds, for a 1 μm laser, to the intensity $I=1.25\times 10^{19}$ W/cm^2. The pulse width is 12λ (the beam is Gaussian in the perpendicular plane and has a Gaussian front). The plasma density corresponds to $\omega_{pe}/\omega=0.6$. The size of the computational box is $40\lambda\times 20\lambda\times 20\lambda$ with ten mesh steps per wavelength and eight electrons and eight ions per cell. The ion to electron mass ratio is equal to $m_i/m_e=1836$.

The relativistic self-focusing of a linearly polarized semi-infinite beam is shown in Fig. 1 at $t=20\times 2\pi/\omega$ (a), $t=45\times 2\pi/\omega$ (b), $t=70\times 2\pi/\omega$ (c). Here a 3D perspective of the isosurface of the electromagnetic energy density is shown at three different times (see also the animations shown in [14]). We see the formation of a narrow self-focusing channel in the region between the leading part of the pulse, with pronounced filamentation, and the wide rear part of the pulse. The laser pulse distortion is asymmetric. This anisotropic self-focusing is illustrated by the projections, shown in Fig. 2, of the isosurface of the electromagnetic energy density W on the (x,z) plane (a) and on the (x,y) plane (b) at $t=60\times 2\pi/\omega$. In the (x,z) plane (which corresponds to the s-polarization plane) the distribution of the electromagnetic energy density is up-down symmetric with three filaments in the leading part of the pulse. The self-focusing in the s plane is very similar to the self-focusing of the s-polarized laser pulse in the 2D case [9]. On the contrary, in Fig. 2(b), the projection on the (x,y) plane (in the p polarization plane) is asymmetric and we see that the leading part of the pulse starts to bend. The pulse bending mechanism is discussed in Ref. [15].

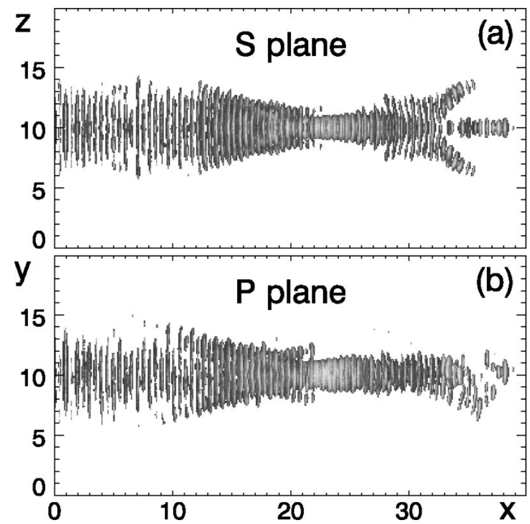

FIG. 2. Projections of the isosurface of the electromagnetic energy density on the (x,z) plane (a) and on the (x,y) plane (b) at $t=60\times 2\pi/\omega$.

The asymmetry of the self-focusing leads to a quite complicated internal structure of the laser pulse channel, as shown in Fig. 3. Here we present two-dimensional cross sections of the distribution of the y component of the magnetic field at $y=10$ (a), of the electron density at $z=10$ (b) and at $y=10$ (c), and of the ion density at $z=10$ (d) and at $y=10$ (e). The self-generated magnetic field [Fig. 3(a)] changes sign in the $z=10$ plane, as discussed in Ref. [9], and its structure corresponds to an electric current density concentrated in the plane $y=10$. In the distribution of the electron and ion densities shown in Figs. 3(b)–3(e), we see a high density thin plasma sheet. Its thickness and width are approximately 1 μm and 4 μm, respectively.

A possible mechanism that can account for the formation of such a sheet is related to the effect of the magnetic field inside the self-focusing channel. As was shown in Ref. [9], the source of the quasistatic magnetic field is the electric current produced by the fast relativistic electrons accelerated in the forward direction. The electric current is directed in the direction opposite to the direction of the light propagation and is localized in the vicinity of the laser pulse axis. The return electric current induced in the plasma flows at the periphery of the self-focusing channel. It is localized in a thin shell at the channel walls. These oppositely directed electric currents repel each other producing a radial expansion of the self-focusing channel and ion heating mostly in the radial direction [16]. On the contrary, in the central region the plasma pinching towards the channel axis prevails. At the initial stage this pinching prevents the ions from expanding radially and, subsequently it leads to the increase of the ion density and to the formation of a high density filament. In the present case the situation is more complex because the quiver motion of the electrons in the plane of the laser electric field contributes substantially to the electron distribution near the channel axis producing the azimuthal anisotropy of the filament. As a result, an ion sheet forms with the shape of a filament elongated in the direction of the laser polarization. We note that in the case of a circularly

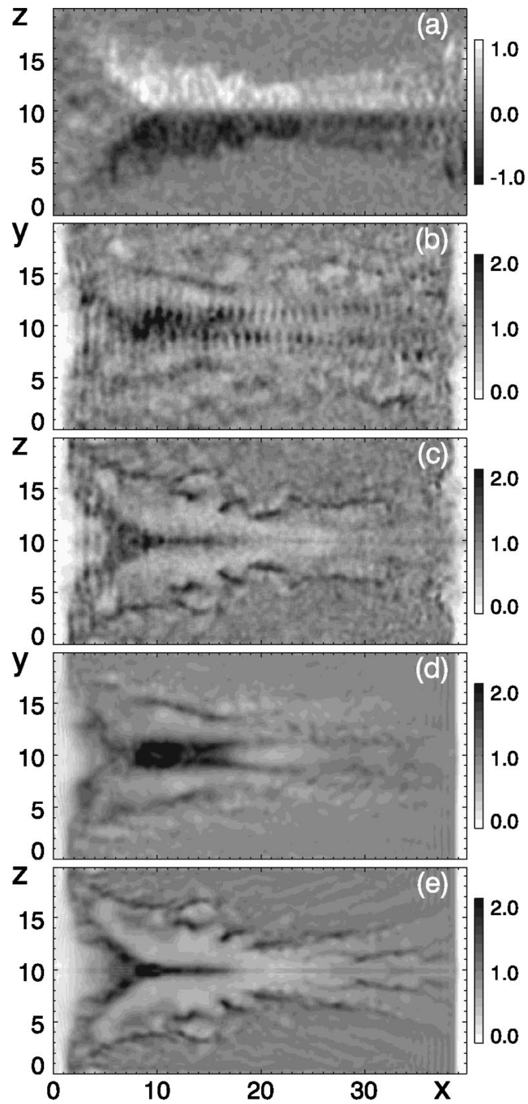

FIG. 3. Cross sections of the distribution of the y component of the magnetic field at $y=10$ (a), of the electron density at $z=10$ (b) and at $y=10$ (c), and of the ion density at $z=10$ (d) and at $y=10$ (e).

polarized laser pulse the filament has a helical form (not shown here). The formation of a plasma layer at the axis of the self-focusing channel plays a key role in the problem of ion acceleration by high intensity laser pulses [17] and provides a way of obtaining high density, strongly collimated jets of high energy ions.

In order to illustrate the properties of ion motion inside the self-focusing channel, in Fig. 4(a) we present the ion trajectories calculated in the 2D case, when an s-polarized

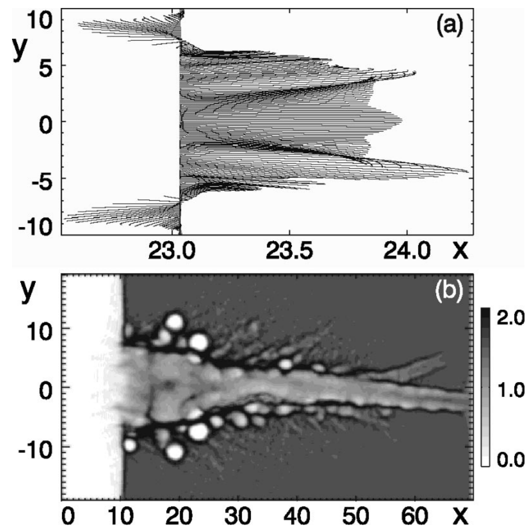

FIG. 4. Ion trajectories inside the self-focusing channel (a) and ion density distribution at $t=120\times 2\pi/\omega$.

laser pulse interacts with an overdense plasma. The dimensionless amplitude of the laser pulse is $a=eE/m_e\omega c=3$. The pulse width is 12λ (the beam is Gaussian in the perpendicular plane and has a Gaussian front). The plasma density corresponds to $\omega_{pe}/\omega=0.6$. We see that the ions at the channel periphery are deflected outwards while the ions localized in the vicinity of the channel axis are not deflected. This results in the formation of the filament seen in the ion density distribution in Fig. 4(b). In this figure we also see the channel shape and the bubbles inside and outside the channel. These bubbles correspond to the post-solitons discussed in detail in Ref. [18].

In conclusion, the different behavior between s and p-polarized pulses [15] implies that the interaction of a linearly polarized pulse in a 3D configuration is strongly anisotropic [10] and exhibits p features in the polarization plane, where the pulse electric field oscillates, and s features in the perpendicular plane, where the pulse magnetic field oscillates. This anisotropy is not controlled by the total pulse power, as is the case for the self-focusing threshold, but by the pulse dimensionless amplitude, being due to a finite orbit size effect in the polarization plane. This asymmetry matches the density asymmetry inside the propagation channel. This channel is not fully void and has a high density sheet aligned along the polarization plane.

We are pleased to acknowledge the use of the Origin SGI 2000 supercomputer at ‘‘Scuola Normale Superiore,’’ Pisa, Italy, and of the Cray T3E at ‘‘Cineca,’’ Bologna, Italy, under the INFM Parallel Computing Initiative.

[1] T. Tajima and J. Dawson, Phys. Rev. Lett. **43**, 262 (1979).

[2] M. Tabak *et al.*, Phys. Plasmas **1**, 1626 (1994); M. Roth *et al.*, Phys. Rev. Lett. **86**, 436 (2001).

[3] G. A. Askar’yan, Zh. Eksp. Teor. Fiz. **42**, 1567 (1962) [Sov. Phys. JETP **15**, 8 (1962)]; Uspekhi Fiz. Nauk **111**, 249 (1973) [Sov. Phys. Usp. **16**, 680 (1973)].

[4] A. G. Litvak, Zh. Eksp. Teor. Fiz. **57**, 629 (1969) [Sov. Phys. JETP **30**, 344 (1969)]; C. Max *et al.*, Phys. Rev. Lett. **33**, 209 (1974); G. Schmidt and W. Horton, Comments Plasma Phys. Control. Fusion **9**, 85 (1985).

[5] G.-Z. Sun *et al.*, Phys. Fluids **30**, 526 (1987); A. B. Borisov *et al.*, Phys. Rev. A **45**, 5830 (1992); X. L. Chen and R. N. Sudan, Phys. Rev. Lett. **70**, 2082 (1993); S. V. Bulanov, F. Pegoraro, and A. M. Pukhov, *ibid.* **74**, 710 (1995).

[6] S. V. Bulanov *et al.*, Phys. Fluids B **4**, 1935 (1992); K.-C. Tseng, W. B. Mori, and C. D. Decker, Phys. Rev. Lett. **76**, 3332 (1996); K. C. Tseng, W. B. Mori, and T. Katsouleas, Phys. Plasmas **6**, 2105 (1999).

[7] S. V. Bulanov *et al.*, IEEE Trans. Plasma Sci. **24**, 393 (1996).

[8] S. V. Bulanov and A. S. Sakharov, Pis'ma Zh. Eksp. Teor. Fiz. 54, 298 (1991) [JETP Lett. **54**, 203 (1991)].

[9] G. A. Askar'yan *et al.*, Pis'ma Zh. Eksp. Teor. Fiz. **60**, 240 (1994) [JETP Lett. **60**, 251 (1994)]; Fiz. Plasmy **21**, 884 (1995) [Plasma Phys. Rep. **21**, 985 (1995)]; Comments Plasma Phys. Control. Fusion **17**, 35 (1995).

[10] T. Honda *et al.*, J. Plasma Fusion Res. **75**, NO10-CD, 219 (1999).

[11] V. E. Zakharov, Zh. Eksp. Teor. Fiz. **62**, 1745 (1972) [Sov. Phys. JETP **35**, 908 (1972)]; E. A. Kuznetsov, A. M. Rubenchik, and V. E. Zakharov, Phys. Rep. **142**, 105 (1986); E. A. Kuznetsov, Chaos **6**, 381 (1996).

[12] T. Zh. Esirkepov, Comput. Phys. Commun. **135**, 144 (2001).

[13] A. Pukhov and J. Meyer-ter-Vehn, Phys. Rev. Lett. **76**, 3975 (1996).

[14] http://staff.mbi-berlin.de/naumova/sf

[15] N. M. Naumova *et al.*, Phys. Plasmas **8**, 4149 (2001).

[16] F. Pegoraro *et al.*, IEEE Trans. Plasma Sci. **28**, 1226P (2000).

[17] T. Zh. Esirkepov *et al.*, Pis'ma Zh. Eksp. Teor. Fiz. **70** 80, (1999) [JETP Lett. **70**, 82 (1999)]; S. V. Bulanov *et al.*, *ibid.* **71**, 593 (2000) [*ibid.* **71**, 407 (2000)]; Y. Sentoku *et al.*, Phys. Rev. E **62**, 7271 (2000); H. Ruhl *et al.*, Fiz. Plazmy **27**, 387 (2001) [Plasma Phys. Rep. **27**, 363 (2001)]; A. V. Kuznetsov *et al.*, *ibid.* **27**, 225 (2001) [*ibid.* **27**, 211 (2001)].

[18] N. M. Naumova *et al.*, Phys. Rev. Lett. **87**, 185004 (2001).